Transactivating mutation of the MYOD1 gene is a frequent event in adult spindle cell rhabdomyosarcoma

Szuhai, K.; Jong, D. de; Leung, W.Y.; Fletcher, C.D.M.; Hogendoorn, P.C.W.

Journal of Pathology
J Pathol 2014; **232:** 300–307
Published online in Wiley Online Library
(wileyonlinelibrary.com) DOI: 10.1002/path.4307

ORIGINAL PAPER

Transactivating mutation of the *MYOD1* gene is a frequent event in adult spindle cell rhabdomyosarcoma

Karoly Szuhai,[1]* Daniëlle de Jong,[1] Wai Yi Leung,[2] Christopher DM Fletcher[3] and Pancras CW Hogendoorn[4]

[1] *Department of Molecular Cell Biology, Leiden University Medical Center, The Netherlands*
[2] *Sequencing Analysis Support Core (SASC), Leiden University Medical Center, The Netherlands*
[3] *Department of Pathology, Brigham and Women's Hospital and Harvard Medical School, Boston, MA, USA*
[4] *Department of Pathology, Leiden University Medical Center, The Netherlands*

**Correspondence to: K Szuhai, Department of Molecular Cell Biology, Leiden University Medical Center, PO Box 9600, Einthovenweg 20, 2330RC Leiden, The Netherlands. e-mail: k.szuhai@lumc.nl*

Abstract

Rhabdomyosarcoma (RMS) is the most common soft-tissue sarcoma in children and adolescents, being characterized by expression of genes and morphological and ultrastructural features of sarcomeric differentiation. The spindle cell variant of rhabdomyosarcoma (spindle cell RMS) in adults has been defined as an entity, separated from embryonal rhabdomyosarcoma (ERMS), with unfavourable clinical outcome. So far, no recurrent genetic alteration has been identified in the adult form of spindle cell RMS. We studied a case of adult spindle cell RMS using next-generation sequencing (NGS) after exome capture. Using this approach, we identified 31 tumour-specific somatic alterations and selected four genes with predicted functional relevance to muscle differentiation and growth. *MYOD1*, *KIF18A*, *NOTCH1*, and *EML5* were further tested for mutations using Sanger sequencing on DNA from FFPE samples from 16 additional, adult spindle cell RMS samples. The highly conserved sequence homology of MYOD1 with other myogenic transcription factors prompted us to screen the basic DNA-binding domains of *MYF5*, *MYF6* and *MYOG* for mutations. From the investigated 17 samples, seven (41%) showed homozygous mutation of *MYOD1*, indicating a critical role in this rare subtype of adult spindle cell RMS, while no mutations were found in any of the other genes involved in myogenic differentiation. The p.L122R mutation occurs in the conserved DNA binding domain in *MYOD1* and leads to transactivation and MYC-like functions. *MYOD1* homozygous mutations are frequent, recurrent and pathognomonic events in adult-type spindle cell RMS.

Keywords: rhabdomyosarcoma; spindle cell; soft tissue tumour; MYOD1; transactivating mutation; next-generation sequencing; bLHL

Received 12 November 2013; Revised 20 November 2013; Accepted 21 November 2013

No conflicts of interest were declared.

Introduction

Rhabdomyosarcoma (RMS) is the most common soft-tissue sarcoma in children and adolescents and is characterized by expression of genes and morphological and ultrastructural features of sarcomeric differentiation. Traditionally, it has been divided into three major subtypes, alveolar (ARMS), embryonal (ERMS) and pleomorphic (PRMS) rhabdomyosarcoma, with multiple histological variants included under the heading of ERMS, comprising spindle cell rhabdomyosarcoma (spindle cell RMS). In the latest *WHO Classification of Tumours of Soft Tissue and Bone,* spindle cell/sclerosing rhabdomyosarcoma has been proposed as a separate entity [1]. Next to histological identification, pathognomonic genetic changes associated with the development of rhabdomyosarcoma are used as ancillary diagnostic tool. Detection of the translocations t(2;13) or t(1;13), giving rise to the *PAX3–FOXO1* or *PAX7–FOXO1* fusions, is used in diagnostic procedures. A subset of histologically identified ARMS lacking these fusions has been identified, with alternative translocations leading to fusions of *PAX3* to *FOXO4, NCOA1* or *NCOA2* or *FOXO1* to *FGFR1* and in about 20% of the histological ARMS cases no translocations have yet been identified [2–4]. In ERMS, so far, only gross genomic alterations have been detected, leading to gain of chromosome 8 and chromosomes 2, 11, 13 and 20, and frequent loss of heterozygosity has been observed at chromosome 11p15.5, but the identification of recurrent translocations or mutations is still awaited [5–7].

Recently, a recurrent gene rearrangement involving the *NCOA2* gene in congenital/infantile spindle cell RMS has been identified in three cases involving *SRF, TEAD1* and a yet-unidentified gene as fusion partners without involvement of *NCOA2* in the remaining 18 childhood and adult cases which were studied. This finding indicates the involvement of other genes and/or

mechanisms in the pathogenesis of childhood or adult spindle cell RMS [8].

In this study we used exome capture-based enrichment of all coding sequence regions of the human genome, analysed by a massively parallel short sequence read approach, to uncover genetic changes involved in the development of adult spindle cell RMS and validate the findings on samples from a larger, histologically well-characterized cohort.

Materials and methods

Patient selection

A 52 year-old male patient with a tumour of the arm showing histological features of spindle cell rhabdomyosarcoma was diagnosed in 2010 at the Leiden University Medical Centre (LUMC), and DNAs isolated from frozen tissue sections (tumour and normal) were used for exome capture sequencing. Formalin-fixed, paraffin-embedded (FFPE) tissue samples were selected for 16 samples diagnosed as adult spindle cell RMS from the archive of CDMF for confirmatory studies. Sample collection and procedures were performed according to the ethical guidelines in the Code for Proper Secondary Use of Human Tissue in The Netherlands (Dutch Federation of Medical Scientific Societies).

DNA isolation and exome sequencing

DNA samples were sequenced at BGI (Beijing, China). In brief, exome capture was carried out using Agilent SureSelect Human All ExonV3 (50 Mb) Kit. Genomic DNA samples were randomly fragmented by Covaris, with a base-pair peak of 150–200 bp, and adapters were ligated to both ends of the fragments. The adaptor-ligated templates were purified using Agencourt AMPure SPRI beads and fragments with insert size 250 bp were excised and amplified by ligation-mediated PCR. The samples were purified and hybridized to the SureSelect Biotinylated RNA Library (BAITS) for enrichment. Captured libraries were loaded onto a HiSeq 2000 platform and paired-end sequencing was performed, with read lengths of 90 bp, which provided at least 50 × average coverage depth for each sample. Raw image files were processed by Illumina base-calling software v 1.7 for base calling with default parameters.

Analysis of exome sequencing data

Standard bioinformatics pipelines established at BGI were used to analyse the data generated at BGI. Sequence result files were subjected to data filtering, removing adaptors contamination and low-quality reads from raw reads. Sequencing data (fastq files) were mapped to the reference genome by BWA (bwa aln-o1-e 50-m100 000-t4-i 15-q10–I). After alignment, the duplicated data were identified using Picard, and result files were generated in BAM format, which were used to visualize aligned reads used as input files in later variant calls detection. Single-nucleotide polymorphisms (SNPs) were identified by OAPsnp (http://soap.genomics.org.cn/soapsnp.html), using the following parameters: soapsnp-t-u-z!-r 0.00005-e 0.0001-QL.

DNA isolation from FFPE samples, gene-specific PCR and Sanger sequencing

Tumour content was estimated using haematoxylin and eosin (H&E)-stained slides and samples with large normal tissue parts were microdissected. In all cases, the estimated tumour content was at least 80%, based on the microscopical evaluation. Due to limited available samples, the genomic DNA from FFPE tissue was isolated from two 10 µm sections, as described previously [9].

Based on the identified mutation list, genes with functional relevance to rhabdomyosarcoma were selected. PCR primers were designed flanking the mutation position with amplicon size of about 100 bp, as confirmatory PCR reactions were performed on DNA isolated from FFPE tissue samples of various origins, with an expected high degree of degradation (Table 2).

PCR amplifications were done using the iQ SYBR green Supermix (Bio-Rad Laboratories, Hercules, CA, USA) and 10 pM M13-tailed primers in a 25 µl final volume on a CFX 96 Real-Time PCR detection system (Bio-Rad). The following PCR conditions were used: initial denaturation step of 5 min at 95 °C, followed by 40 cycles of 10 s at 95 °C, 10 s at 60 °C and 30 s at 72 °C. Purified PCR products were sequenced using Sanger sequencing methods, using standard M13 reverse and forward primers by Macrogen (Amsterdam, The Netherlands). Resulting sequence files were further analysed using Mutation Surveyor DNA Variant Analysis software v 3.97 (SoftGenetics, UK).

Results

Patient characteristics

We observed homozygous mutations of *MYOD1* in seven of the 17 cases investigated (41%). The mean age of the investigated patient group was 48 (range 20–80) years and patients with mutations showed a lower mean age, 41 (range 20–71) years and a similar distribution. For gender distribution, the group consisted of eight male and nine female patients, from whom mutations were detected in four males and three females. With regard to localization, two cases were in the head and neck region, one on the trunk and four in the extremities (three lower limb, one upper limb). Patient characteristics, including available follow-up, are given in Table 1.

Table 1. Patient characteristics of immunohistochemical and MYOD1 mutation results

Case no.	Age (years)/ sex	Location	MYOD1 L122R Mut	IHC-positive	IHC-focal positive	IHC-negative
1	52/M	Left arm	+	DES, MYF4,		SMA, CALD, CD34, S100
2	32/F	Left thigh	+	DES	fMYOS	S100, SMA
3	28/M	Thigh	+	HHF35, SMA		S100, GFAP, CALD
4	71/F	Right lower leg	+	DES, MYF4		
5	54/M	Tongue	–	DES, MYF4	SMA	
6	80/F	Left thigh	–	DES, MYF4, HHF35, S100		S100, GFAP
7	24/M	Pharynx	+	DES, MYF4	SMA	S100, GFAP
8	70/M	Neck	–	DES, MYF4	SMA	S100, GFAP, CD34, CD31, CALD
9	41/M	Maxillary sinus	–	DES, MYF4	AE1/AE3	S100, PAN-K, MART1, HMBA45
10	32/F	Vulva	–	DES, MYF4	TLE1-nucl	S100, GFAP, CALD, CD34, EMA, AE1/AE3
11	36/F	Tongue	–	DES, MYF4	SMA	S100, CALD, P63, PAN-K
12	48/F	Neck	–	DES, MYF4		SMA, CALD, EMA, AE1/AE3, S100, GFAP, TLE1
13	20/F	Mouth	+	DES, MYF4	SMA	S100, PAN-K
14	61/F	Mouth	–	DES, MYF4, PAN-K		CALD, S100, P63
15	64/M	Left hip	+	DES, MYF4, HHF34, MYOS		SMA, CALD
16	52/M	Neck	–	DES, MYF4	SMA	SMA, CALD, S100, CD34
17	53/F	Leg	–	DES, MYF4, HHF35, CAM5.2	AE1/AE3	SMA, CALD, S100, MART1

Histopathology

All cases were reviewed by expert soft tissue pathologists (CDMF, PCWH) and fulfilled the histological criteria put forward in the latest WHO fascicle for spindle cell rhabdomyosarcoma [1]. Representative histological images of spindle cell RMS are shown in Figure 1, with the typical morphological appearance of two cell populations. The dominant neoplastic cell population consists of spindle cells forming long, intersecting fascicles, with small oval to elongated nuclei, inconspicuous to small nucleoli and pale indistinct cytoplasm. A small number of cells, significant for establishment of the diagnosis, are rounded or elongated rhabdomyoblasts with hyperchromatic, eccentrically placed nuclei and abundant, brightly eosinophilic cytoplasm scattered throughout the tumour (Figure 1B). Frequent mitoses were noted. The skeletal muscle lineage of these tumours can be confirmed by immunohistochemical studies, showing positive staining for desmin, myf-4, fast-myosin or myoglobin, with myf-4 having the highest sensitivity (Table 1).

NGS results

After analysis of the derived BAM files, a mutation report was generated from exome sequencing from normal and tumour tissue-derived DNA, resulting in 9333 and 9126 mutations, respectively. Nucleotide changes were then further filtered, removing single nucleotide polymorphisms located in intergenic regions, intronic regions without affecting splicing, and exonic regions leading synonymous mutations leaving the amino acid code unchanged. In addition, mutations that were present in a heterozygous state in the normal tissue, and which reverted to complete wild-type or remained in a heterozygous state, were excluded. After applying all these filters, a list of gene mutations was generated. This list was then further stratified based on prediction for potential functional relevance with regard to gain or loss of protein function, using Mutation Taster [10], and were further filtered against the 1000 genome SNP database to exclude alterations occurring at high frequency in the normal population, and checked data were entered into the COSMIC database. After filtering, 31 genes were then selected (Table 3), consisting of one splice site mutation, two homozygous mutations, one mitochondrial DNA (mtDNA) mutation and 27 heterozygous mutations, all gained *de novo* when compared to the sequences obtained from normal tissue. As an example, the detected homozygous *MYOD1* mutation (*MYOD1* c.365 T >G, p.L122R) is shown in Figure S1 (see supplementary material).

From this gene list, based on its functional likelihood in muscle and/or tumour development, five genes were selected for sequence verification using Sanger sequencing. This set of genes was then further used to test the presence of mutation in a set of well-characterized adult spindle cell rhabdomyosarcoma samples. From the COSMIC database v 67 (http://

Table 2. Primer sequences used in Sanger sequencing reactions

Primer name	Sequence*
F_MYOD1	5′-*TGTAAAACGACGGCCAGT*CAAGCGCAAGACCACCAAC-3′
R_MYOD1	5′-*CAGGAAACAGCTATGACC*GGTTTGGATTGCTCGACGTG-3′
F_NOTCH1	5′-*TGTAAAACGACGGCCAGT*GTGTGACCAGCACGGCA-3′
R_NOTCH1	5′-*CAGGAAACAGCTATGACC*GAGGGGGATGTCAACGAGTG-3′
F_KIF18A	5′-*TGTAAAACGACGGCCAGT*TGCTATTCTAACAGGGAAAAAG ATG-3′
R_KIF18A	5′-*CAGGAAACAGCTATGACC*CACTTGCTGTCCGGGAAGAT-3′
F_XRCC1	5′-*TGTAAAACGACGGCCAGT*GGTACAGCTTACCTGGGACG-3′
R_XRCC1	5′-*CAGGAAACAGCTATGACC*GACTCCCCCTTTGGCTTGAG-3′
F_EML5	5′-*TGTAAAACGACGGCCAGT*TCATCAGCTGTAACTAAAACTT GGC-3′
R_EML5	5′-*CAGGAAACAGCTATGACC*TGTTTCAGGCCTTGAAGTAAA TGG-3′
F_MYOG	5′-*TGTAAAACGACGGCCAGT*AAGAGGAAGTCGGTGTCCGT-3′
R_MYOG	5′-*CAGGAAACAGCTATGACC*GTTGAGCAGGGTGCTTCTCT-3′
F_MYF5	5′-*TGTAAAACGACGGCCAGT*TGCAAGAGGAAGTCCACCAC-3′
R_MYF5	5′-*CAGGAAACAGCTATGACC*CCTCTGGTTGGGGTTGGTC-3′
F_MYF6	5′-*TGTAAAACGACGGCCAGT*GAGAAAATCTGCCCCCACTGA-3′
R_MYF6	5′-*CAGGAAACAGCTATGACC*CAGCCTCTGGTTGGGGTTG-3′

*Italic underlined parts represent M13 forward or M13 reverse sequences.

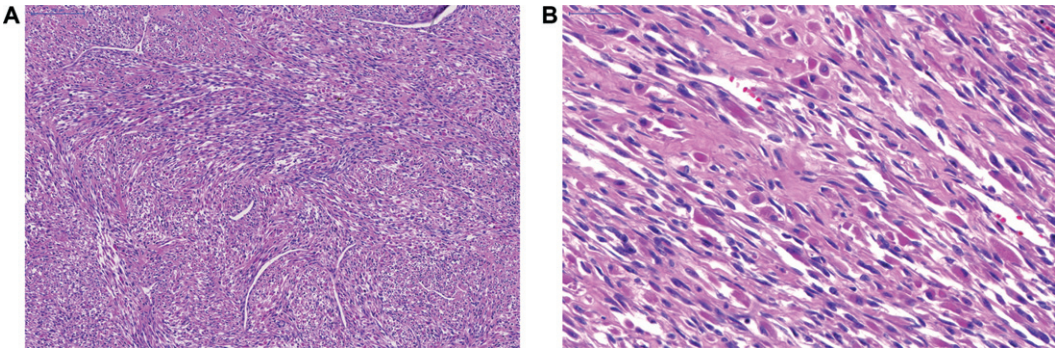

Figure 1. Representative histological image after H&E staining of spindle cell rhabdomyosarcoma. (A) The dominant neoplastic cell population consists of spindle cells forming long, intersecting fascicles with small oval to elongated nuclei (×10 magnification). (B) Polygonal rhabdomyoblasts with hyperchromatic, eccentrically placed nuclei and abundant bright eosinophilic cytoplasm scattered throughout the tumour. Spindle cells show inconspicuous to small nucleoli and pale indistinct cytoplasm (×40 magnification).

Table 3. List of identified mutation by using next generation sequencing after exome capture

Chromosome no.	Chromosome position	Gene name	Reference nucleotide	Tumour mutation call	Mutation Taster classification	Mutation Taster score	1000 Genomes frequency
1	149903181	*MTMR11*	G	A	D	0·9753	NA
1	171557531	*PRRC2C*	A	G	D	**0.9965**	NA
3	72428580	*RYBP*	T	C	SPLICE	**NA**	NA
4	42122254	*BEND4*	C	G	D	**0.99999**	NA
7	6485734	*DAGLB*	A	C	D	0·9348	NA
7	151843688	*MLL3*	T	C	D	0·9984	NA
9	79117520	*GCNT1*	C	G	D	0·9234	NA
9	138742011	*CAMSAP1*	C	A	D	**0.9999**	NA
9	139401228	***NOTCH1***	T	A	D	0·9987	NA
9	139907251	*ABCA2*	A	C	D	0·9972	NA
10	5138714	*AKR1C3*	G	A	D	0·8206	NA
10	7749183	*ITIH2*	C	T	D	0·9159	0.0335
11	6623433	*RRP8*	G	A	D	0·9397	NA
11	10650367	*MRVI1*	G	A	D	**0.9996**	NA
11	14991605	*CALCA*	T	C	D	0·6915	NA
11	17741694	***MYOD1***	T	G	D	1	NA
11	28112979	***KIF18A***	C	T	D	0·9598	NA
12	49427860	*MLL2*	T	C	D	**0.9996**	NA
12	54348800	*HOXC12*	C	G	D	0·9717	NA
14	60976537	*SIX6*	C	A	D	0·9944	0.4458
14	61518550	*SLC38A6*	T	C	D	0·9947	NA
14	68193731	*RDH12*	G	A	D	0·629	0.0714
14	74404756	*FAM161B*	T	C	D	0·5878	0.4358
14	81970587	*SEL1L*	A	G	D	0·9996	NA
14	89178711	***EML5***	T	C	D	**0.99037**	NA
15	57967247	*GCOM1*	G	C	D	**0.9844**	NA
16	55862691	*CES1*	G	A	D	0·6109	0.2849
19	44057805	***XRCC1***	A	C	D	0·977	NA
20	744193	*C20orf54*	C	T	D	0·9993	NA
21	47722067	*C21orf58*	T	C	D	0·7423	NA
M	15306	*CYTB*	T	C	NA	**NA**	NA

Genes in bold were verified by Sanger sequencing.
NA, not available; D, deleterious effect.

cancer.sanger.ac.uk/cancergenome/projects/cosmic/), mutation data were retrieved from >200 rhabdomyosarcoma samples, including ARMS, ERMS, mixed RMS, pleomorphic RMS and one sclerosing RMS. None of the RMS cases entered into COSMIC showed identical mutation to those detected by us, *MYOD1* or *NOTCH1* or any other genes investigated herein. In the COSMIC database, mutations of the RAS gene family (*HRAS, KRAS, NRAS*) were found, with *NRAS* mutation as the most frequent event in ERMS. However, our full-exome sequenced case showed no mutation in any of these genes. Investigating the presence of *MYOD1* mutation at p.L122 for all tumour entities entered into the COSMIC database, we identified two lung cancer cases, one with p.L122L; c366G>A (synonymous mutation) and one with p.L122M; c.364C>A, non-identical to the mutation detected by us. It is likely that MYOD1 has no functional activity in lung cancer and therefore can be regarded as a passenger mutation.

PCR verification

Based on the NGS results, five genes were selected for further verification in multiple tumour samples (*MYOD1, NOTCH1, KIF18A, XRCC5* and *EML5*). PCR primers bracketing the mutation position, resulting in short amplified DNA segments, were used for the FFPE-isolated DNA samples and were subjected to Sanger sequencing, using fluorescence-based detection and capillary sequencing. Amplified PCR products resulted in good-quality sequence reads and were interpretable in all cases analysed. A homozygous mutation was detected for the genes *MYOD1* and *KIF18A,* a heterozygous mutation was detected for the genes *EML5* and *NOTCH1,* confirming the NGS data, but heterozygous mutation of the gene *XRCC5* was not detected in case 1 (L3230). Sixteen samples of adult SCRMS cases were selected for additional PCR reactions. Mutations at sequence positions identified by NGS were not detected for *NOTCH1, EML5, KIF18A* or *XRCC5* in any of the investigated cases. A homozygous mutation of the *MYOD1* gene was detected in six of 16 cases, thus seven being identified in total out of the 17 (41%) cases investigated (Figure 2, Table 1). The family of myogenic transcription factors with bHLH shows a very high degree of conservation at the protein level, therefore we performed sequencing of the DNA binding domain region of MYF5, MYF6 and MYOG corresponding to the mutation position in *MYOD1* (Figure 3). A mutation at a position corresponding to p.L122 of MYOD1, leading to a p.L122R change, could potentially be responsible in the remaining spindle cell RMS cases. Short sequences were amplified and analysed by Sanger sequencing from the 10 *MYOD1* mutation-negative cases for the genes *MYF5, MYF6* and *MYOG*. Mutations related to this position were absent in all cases investigated.

Discussion

Spindle cell RMS, as a distinct entity occurring in children, was first described by Cavazzana *et al.* [11], based on data obtained from the German–Italian Cooperative Study (GICS), and its existence was confirmed by Leuschner *et al.* [12], based on data obtained from the Intergroup Rhabdomyosarcoma Studies (IRS) I and II. A dominant male:female ratio, paratesticular localization and better prognosis were the major landmarks associated with this entity. In 1998 Rubin *et al.* described spindle cell RMS cases affecting adults, and their findings were validated in multiple cases by Nascimento *et al,* Mentzel *et al.* and Stock *et al.* [13–16]. In contrast to childhood spindle cell RMS, adult tumours have poorer prognosis and they exhibit a broader morphological spectrum, including sclerosing and pseudovascular types.

We used a massively parallel sequencing approach to interrogate the whole human genome coding sequences after a hybrid capture method in an index case with histo-morphological appearances of adult spindle cell RMS. As a reference we used DNA isolated from normal tissue from the same individual. Sequences were then compared to each other and to reference database to filter out potentially non-pathogenic mutations. With NGS we detected one splice site, two homozygous (*MYOD1, KIF18A*), one mtDNA and 27 heterozygous mutations. The two homozygous mutations (*MYOD1, KIF18a*) detected were located on chromosome 11 and, based on copy number loss of heterozygosity (LOH), we observed a copy number-neutral LOH involving the short arm of chromosome 11p14.1–15.5. Mutations in *IGF2, HRAS* or *p57* (*KIP2*), all of which reside on the short arm of chromosome 11 and which are implicated in the pathogenesis of ERMS, were not detected [6,7]. Based on functional relevance to muscle differentiation, we have selected five genes and designed primer pairs for short amplicons for sequencing from FFPE samples and validated on a set of adult SCRMS from 16 cases (Table 1). All but one mutation were confirmed using Sanger sequencing in the index case. A recurrent mutation of *MYOD1* c.365 T > G, p.L122R was found in six additional cases, resulting in a *MYOD1* mutation rate of 41% (seven of 17 cases) in adult spindle cell RMS.

MYOD1 (also known as *MYOD*) is member of the basic helix–loop–helix (bHLH) family of transcription factors and the myogenic factors subfamily, also known in the literature as myogenic regulatory factors (MRFs). It plays a key role in skeletal muscle determination and differentiation, together with other bHLH genes *MYF5, MYF6* (also known as *Herculin* and *MRF4*) and *MYOG* (also known as *myogenin* or *MYF4*). The bHLH domains consist of 12–15 amino acid segments consisting of basic residues and a region consisting of two amphipathic α-helixes of approximately 15 amino acids each [17].

The basic domain is responsible for the sequence-specific DNA binding function, recognizing E-box sites (CANNTG) located in the promoter region of muscle-specific genes. The basic domain of *MYOD1* shows 100% homology to the basic domain of MYF5 and has a single amino acid difference as compared to *MYOG* and *MYF6* (Figure 3). Conservation of two amino acids in the basic domain of *MYOD1* (Ala114 and Thr115) and *MYC* has led to investigation into the effect of amino acid substitutions of *MYOD1* at various positions. From the nine amino acid substitutions, mutation of Leu 122 to Arg in *MYOD1* conferred reduced transcriptional activation at *MYOD1* sites, together with enhanced binding to *MYC* sites [17]. The role of a single nucleotide substitution, CTG > CGG, leading to p.L122R amino acid substitution, was a conceivable mechanism in skeletal muscle oncogenesis. In a follow-up study by Anand *et al.* [18], the authors investigated the presence of a possible *MYOD1,* or *MYF5* or *MYF6* or *MYOG* transactivating mutation in 19 RMS samples (13 ERMS, 6 ARMS) and 14 RMS cell lines (7 ERMS, 6 ARMS) and found no mutation in any of the 33 cases investigated. We were

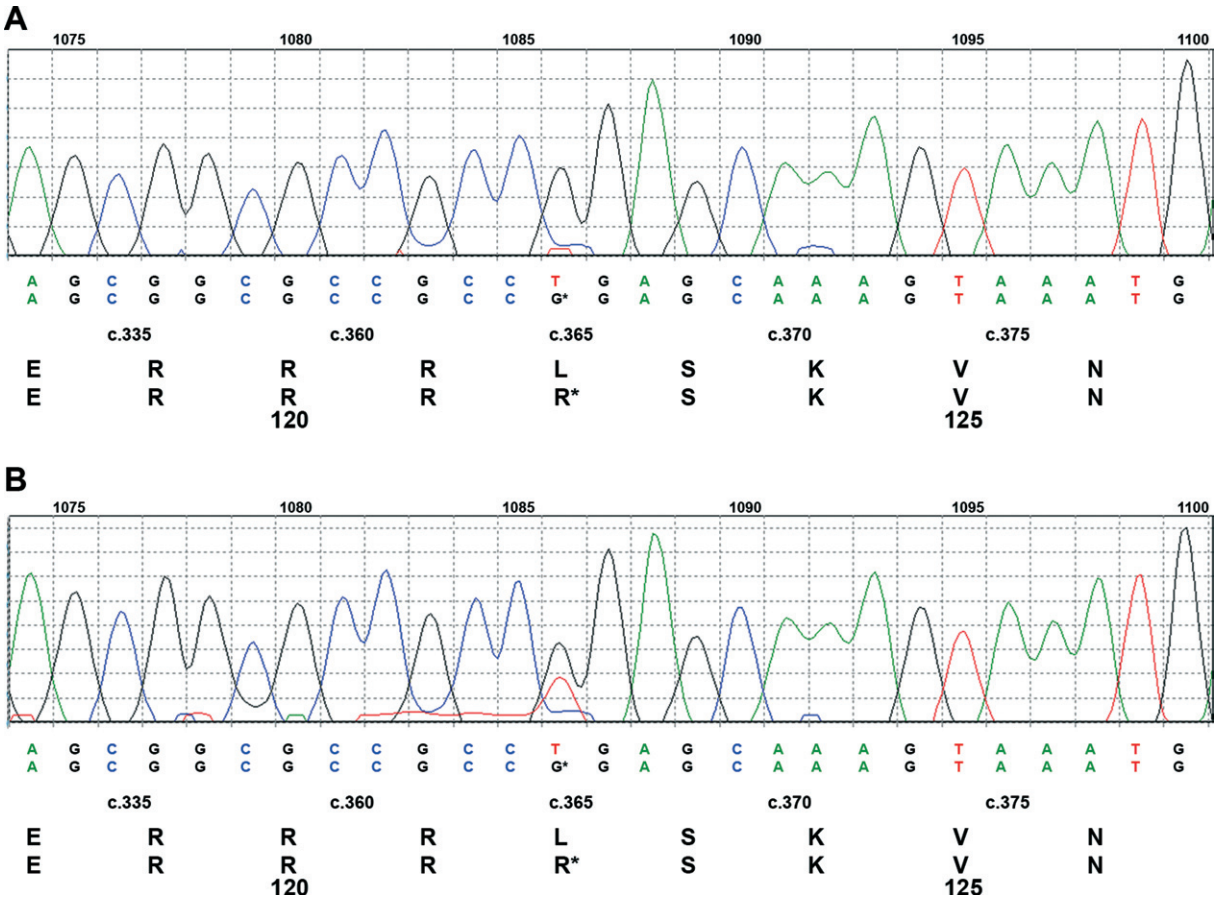

Figure 2. Sanger sequencing verifies the presence of *MYOD1* mutation in case 1 (L3230; A) and case 3 (B). The presence of a *MYOD1* c.365T > G, p.L122R is clearly visible. In (B) the presence of a wild-type peak is caused by the normal tissue in the section, as the mutation load is greater than the expected value of 50%.

```
                                                    L122R
P15172/MYOD1/aa109-125  D R R K A A T M R E R R R L S K V
P13349/MYF5/aa83-99     D R R K A A T M R E R R R L K K V
P23409/MYF6/aa93-109    D R R K A A T L R E R R R L K K I
P15173/MYOG/aa81-97     D R R R A A T L R E K R R L K K V
P01106/MYC/aa354-370    V K R R T H N V L E R Q R R N E L
                          *             *     * :
```

Figure 3. Clustal alignment of at the DNA binding domain of bHLH myogenic transcription factors and Myc. UniProtKB, protein name, amino acid position inside the respectively referred protein sequence: *completely conserved position; mutated position marked as :

unable to identify the pathognomonic transactivating *MYOD1* and other MRFs mutation in >200 cases of RMS entered into the COSMIC database, including one case of sclerosing RMS. The recently reported, recurrent *NCOA2* translocation was present exclusively in congenital/infantile spindle cell RMS and was absent in 18 cases of spindle cell RMS from children, adolescent or adults, pointing to genetically different entities with similar histomorphological appearances [8]. In our study, we specifically selected spindle cell RMS from adults and used stringent histopathological criteria for inclusion [1]. Using Sanger sequencing, we identified a homozygous *MYOD1* c.365 T >G, p.L122R mutation in six additional cases, indicating that the presence of mutation might act as a key factor in skeletal muscle oncogenesis. Based on the functional homologies, in addition to *MYOD1*, we sequenced the basic domain coding region in *MYF5, MYF6* and *MYOG* of all *MYOD1* mutation-negative cases. A yet-unidentified factor that might result in similar functional mimicry might be responsible in cases without mutation at the DNA binding region of various myogenic transcription factors (*MYOD1, MYF5, MYF6* and *MYOG*). This transactivating mutation mechanism does not exclude the existence of chromosomal rearrangements leading to a gene fusion involving MRFs, resulting in a similar functional switch in the mutation-negative cases.

Notch signalling plays an important role in myogenic differentiation by inducing expression of the hairy enhancers of split (HES) family of bHLH

proteins. Cooperative oncogenic activation resulting from constant activation of *NOTCH1,* caused by its mutation in combination with the transactivating *MYOD1* mutation, seemed to be an appealing mechanism, as we observed the *NOTCH1* mutation in our index case [19]. However, sequencing of *NOTCH1* and other candidate genes identified by NGS after exome capture has revealed no mutation in any of the other 16 cases examined. The lack of these mutations in all other spindle cell RMS cases, including the *MYOD1* mutation-negative cases, indicates that these mutations were most likely secondary events during tumour formation and were not acting as driver genes. Comparing *MYOD1* c.365 T >G, p.L122R mutation-negative and -positive cases with regard to classical clinicopathological features (gender, location, immunohistochemistry), we were unable to find any difference between these two groups.

The myogenic bHLH transcription factors regulate skeletal muscle specification and differentiation. MYOD1 and MYF5 are expressed in replicating myoblasts, acting as transcriptional activators as heterodimers with E-proteins and with other bHLH transcription factors, such as MYC and MAX [20]. During terminal differentiation, withdrawal of MYC expression is necessary to prevent cell cycling. In a model system by van Antwerp and colleagues [17] it has been shown that the *MYOD1* c.365 T >G, L122R mutation confers MYC-like activity. The *MYOD1* mutation detected by us likely imparts *MYC* function, resulting in sustained proliferation and an early block of the myogenic differentiation process, leading to the observed spindle cell morphology and some degree of sarcomeric differentiation.

It is now a well-recognized fact that specific genetic changes are often associated with distinct histomorphological features. In this regard, in most the recent WHO classification [1], spindle cell RMS is no longer regarded as a variant of ERMS and, based on histomorphological and clinical differences, is now listed as a separate category of RMS, along with sclerosing RMS. Our data, along with those of Mosquera *et al.* [8], further support this reclassification. Data available so far suggest that infantile and adult subsets of spindle cell RMS are genetically distinct, but the status of 'conventional' paediatric spindle cell RMS remains uncertain in this regard. The presence of a recurrent transactivating mutation in adult spindle cell RMS underlines the potential importance of molecular testing alongside the histopathological diagnosis. Adult-type rhabdomyosarcoma may form a different spectrum involving spindle cells, mixed and pleomorphic types, as proposed by Stock *et al.* [16]; however, the role of *MYOD1* mutation in these entities has yet to be established. Additional studies will potentially stratify the mutation-negative and -positive cases in clinical settings. The possibility of generating small molecules that inhibit the transactivation function of mutant *MYOD1* may offer a novel treatment possibility for this tumour entity.

In conclusion, we describe a recurrent *MYOD1* mutation involving the DNA-binding domain that imparts MYC-like function, as predicted in model systems, occurring specifically in 41% of adult spindle cell RMS.

Acknowledgements

This project was sponsored by the Leiden University Fund (LUF) and Den Dulk Moermans Fonds. The authors would like to thank Pauline Wijers-Koster and Hailang Mei.

Author contributions

KS, PCWH and CDMF conceived experiments; KS, DJ and WYL conceived and carried out experiments and analysed data. All authors were involved in writing the paper and had final approval of the submitted and published versions.

References

1. Nascimento AF, Barr FG. Spindle cell/Sclerosing rhabdomyosarcoma. In *WHO Classification of Tumours of Soft Tissue and Bone*, Fletcher CDM, Bridge JA, Hogendoorn PCW, Mertens F (eds). IARC: Lyons, 2013; 134–135.
2. Sorensen PH, Lynch JC, Qualman SJ, *et al. PAX3–FKHR* and *PAX7–FKHR* gene fusions are prognostic indicators in alveolar rhabdomyosarcoma: a report from the children's oncology group. *J Clin Oncol* 2002; **20:** 2672–2679.
3. Kikuchi K, Rubin BP, Keller C. Developmental origins of fusion-negative rhabdomyosarcomas. *Curr Top Dev Biol* 2011; **96:** 33–56.
4. Parham DM, Barr FG. Alveolar rhabdomyosarcoma. In *WHO Classification of Tumours of Soft Tissue and Bone*, Fletcher CDM, Bridge JA, Hogendoorn PCW, Mertens F (eds). IARC: Lion, 2013; 130–132.
5. Williamson D, Missiaglia E, de Reynies A, *et al.* Fusion gene-negative alveolar rhabdomyosarcoma is clinically and molecularly indistinguishable from embryonal rhabdomyosarcoma. *J Clin Oncol* 2010; **28:** 2151–2158.
6. Davicioni E, Anderson MJ, Finckenstein FG, *et al.* Molecular classification of rhabdomyosarcoma – genotypic and phenotypic determinants of diagnosis: a report from the Children's Oncology Group. *Am J Pathol* 2009; **174:** 550–564.
7. Parham DM, Barr FG. Embryonal rhabdomyosarcoma. In *WHO Classification of Tumours of Soft Tissue and Bone*, Fletcher CDM, Bridge JA, Hogendoorn PCW, Mertens F (eds). IARC: Lyons, 2013; 127–129.
8. Mosquera JM, Sboner A, Zhang L, *et al.* Recurrent *NCOA2* gene rearrangements in congenital/infantile spindle cell rhabdomyosarcoma. *Genes Chromosomes Cancer* 2013; **52:** 538–550.
9. de Jong D, Verbeke SL, Meijer D, *et al.* Opening the archives for state of the art tumour genetic research: sample processing for array-CGH using decalcified, formalin-fixed, paraffin-embedded tissue-derived DNA samples. *BMC Res Notes* 2011; **4:** 1.
10. Schwarz JM, Rodelsperger C, Schuelke M, *et al.* MutationTaster evaluates disease-causing potential of sequence alterations. *Nat Methods* 2010; **7:** 575–576.
11. Cavazzana AO, Schmidt D, Ninfo V, *et al.* Spindle cell rhabdomyosarcoma. A prognostically favorable variant of rhabdomyosarcoma. *Am J Surg Pathol* 1992; **16:** 229–235.

12. Leuschner I, Newton WA Jr, Schmidt D, *et al.* Spindle cell variants of embryonal rhabdomyosarcoma in the paratesticular region. A report of the Intergroup Rhabdomyosarcoma Study. *Am J Surg Pathol* 1993; **17:** 221–230.
13. Rubin BP, Hasserjian RP, Singer S, *et al.* Spindle cell rhabdomyosarcoma (so-called) in adults: report of two cases with emphasis on differential diagnosis. *Am J Surg Pathol* 1998; **22:** 459–464.
14. Nascimento AF, Fletcher CDM. Spindle cell rhabdomyosarcoma in adults. *Am J Surg Pathol* 2005; **29:** 1106–1113.
15. Mentzel T, Kuhnen C. Spindle cell rhabdomyosarcoma in adults: clinicopathological and immunohistochemical analysis of seven new cases. *Virchows Arch* 2006; **449:** 554–560.
16. Stock N, Chibon F, Binh MB, *et al.* Adult-type rhabdomyosarcoma: analysis of 57 cases with clinicopathologic description, identification of three morphologic patterns and prognosis. *Am J Surg Pathol* 2009; **33:** 1850–1859.
17. Van Antwerp ME, Chen DG, Chang C, *et al.* A point mutation in the *MyoD* basic domain imparts c-Myc-like properties. *Proc Natl Acad Sci USA* 1992; **89:** 9010–9014.
18. Anand G, Shapiro DN, Dickman PS, *et al.* Rhabdomyosarcomas do not contain mutations in the DNA binding domains of myogenic transcription factors. *J Clin Invest* 1994; **93:** 5–9.
19. Kuroda K, Tani S, Tamura K, *et al.* Delta-induced Notch signaling mediated by RBP-J inhibits MyoD expression and myogenesis. *J Biol Chem* 1999; **274:** 7238–7244.
20. Yang Z, MacQuarrie KL, Analau E, *et al.* MyoD and E-protein heterodimers switch rhabdomyosarcoma cells from an arrested myoblast phase to a differentiated state. *Genes Dev* 2009; **23:** 694–707.

SUPPLEMENTARY MATERIAL ON THE INTERNET

The following supplementary material may be found in the online version of this article:

Figure S1. A sequence read overview of the resulted NGS read for case 1.